

# Measuring Directed Triadic Closure with Closure Coefficients

Hao Yin  
Stanford University  
yinh@stanford.edu

Austin R. Benson  
Cornell University  
arb@cs.cornell.edu

Johan Ugander  
Stanford University  
jugander@stanford.edu

## ABSTRACT

Recent work studying clustering in undirected graphs has drawn attention to the distinction between measures of clustering that focus on the “center” node of a triangle vs. measures that focus on the “initiator,” a distinction with considerable consequences. Existing measures in directed graphs, meanwhile, have all been center-focused. In this work, we propose a family of *directed closure coefficients* that measure the frequency of triadic closure in directed graphs from the perspective of the node initiating closure. We observe dramatic empirical variation in these coefficients on real-world networks, even in cases when the induced directed triangles are isomorphic. To understand this phenomenon, we examine the theoretical behavior of our closure coefficients under a directed configuration model. Our analysis illustrates an underlying connection between the closure coefficients and moments of the joint in- and out-degree distributions of the network, offering an explanation of the observed asymmetries. We use our directed closure coefficients as predictors in two machine learning tasks. We find interpretable models with AUC scores above 0.92 in class-balanced binary prediction, substantially outperforming models that use traditional center-focused measures.

## 1 INTRODUCTION

A fundamental property of networks across domains is the increased probability of edges existing between nodes that share a common neighbor, a phenomenon known as clustering or triadic closure [38, 46]. These concepts underpin various ideas in the study of networks—especially in undirected network models with symmetric relationships—including the development of generative models [19, 24, 40, 42], community detection [10, 14], and feature extraction for network-based machine learning tasks [16, 21].

A standard measure for the frequency of triadic closure on undirected networks is the *clustering coefficient* [5, 45, 46]. At the node level, the *local clustering coefficient* of a node  $u$  is defined as the fraction of wedges (i.e., length-2 paths) with center  $u$  that are closed. This means that there is an edge connecting the two ends of the wedge, inducing a triangle. At the network level, the *average clustering coefficient* is the mean of the local clustering coefficients [46], and the *global clustering coefficient*, also known as *transitivity* [5], is the fraction of wedges in the entire network that are closed.

Recent research has pointed out a fundamental gap between how triadic closure is measured by the clustering coefficient and how it is usually explained [48]. Local clustering is usually explained by some transitive property of the relationships that edges represent; for social networks this is embodied in the idea that “a friend of my friend is my friend” [19]. In these explanations, however, triadic closure is driven not by the center of a length-2 path but rather by an end node (which we refer to as the *head*), who initiates a new connection. In contrast, the local clustering coefficient that measures triadic closure from the center of a wedge implicitly

accredits the closure to the center node. The recently proposed *local closure coefficient* closes this definitional gap for undirected graphs by measuring closure with respect to the fraction of length-2 paths starting from a specified head node that are closed [48].

The clustering and closure coefficients are only defined on undirected networks. However, in many real-world networks, interactions are more accurately modeled with an associated orientation or direction. Examples of such networks include food webs, where the direction of edges represents carbon or energy flow from one ecological compartment to another; hyperlink graphs, where edges represent which web pages link to which others; and certain online social networks such as Twitter, where “following” relationships are often not reciprocated. The direction of edges may reveal underlying hierarchical structure in a network [3, 8, 17], and we should expect the direction to play a role in clustering.

Extensions of clustering coefficients have been proposed in directed networks [9, 43], which are center-based at the node level. However, measuring directed clustering from the center of a wedge is even less natural in the directed case, while measuring from the head is a more common description of directed closure relationships. For example, in citation networks, paper  $A$  may cite  $B$ , which cites  $C$  and leads  $A$  to also cite  $C$ . In this scenario, the initiator of this triadic closure is really paper  $A$ . Measuring clustering from  $A$  would be the analog of the *closure coefficient* for directed networks, which is what we develop in this paper.

**The present work: directed closure coefficients.** Here we propose a family of directed closure coefficients, which are natural generalizations of the closure coefficients for undirected networks. Like the undirected version of closure coefficients, these measures are based on the head node of a length-2 path, in agreement with common mechanistic interpretations of directed triadic closure and fundamentally different from the center-based clustering coefficient. For example, in citation networks, reading and citing one paper usually leads to reading its references and subsequent citations [47]; and in directed social networks, outgoing edges may represent differential status [3, 23], where if person  $u$  thinks highly of  $v$  and  $v$  thinks highly of  $w$ , then  $u$  is likely to think highly of person  $w$  and consequently initiate an outbound link.

We start by defining a *directed wedge* as an ordered pair of directed edges that share a common node, and the “non-center” end nodes of this wedge on the first and second edge are called the *head* and *tail* nodes, respectively (in Fig. 1, solid lines mark the wedge, where node  $u$  is the head and node  $w$  is the tail). Since each edge may be in either direction, there are four wedge types. When considering triadic closure for each wedge type, the closing edge between the head and tail nodes may also take either direction. Therefore, at each node, there are eight local directed closure coefficients, each representing the frequency of directed triadic closure with a certain wedge type and closure direction (Figure 1). Analogous to the undirected case, we also define the average and

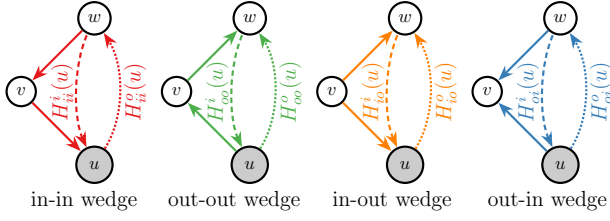


**Figure 1: Illustration of four wedge types and eight local directed closure coefficients at node  $u$ . The type of wedge is denoted by two letters: the first and second letters represent the direction of the edges with respect to the head node  $u$  and the center node  $v$ , respectively. A wedge is  $i$ -closed if there is an incoming edge to the head node from the tail, and  $o$ -closed if there is an outgoing edge from the head node to the tail. There are eight local directed closure coefficients at node  $u$ , denoted as  $H_{xy}^z(u)$  with  $x, y, z \in \{i, o\}$ . Each local directed closure coefficient measures the frequency of triadic closure of a certain wedge type (denoted by subscript  $xy$ ) and closing direction (denoted by superscript  $z$ ).**

global directed closure coefficients to measure the overall frequency of triadic closure in the entire network. These metrics provide a natural and intuitive way to study the frequency of directed triadic closure in details and in particular to measure how directions of the incident and second edge influence a node’s tendency to initiate or receive directed triadic closure.

Our empirical evaluations of the directed closure coefficients on real-world networks reveal several interesting patterns. At the node level, we find clear evidence of a 2-block correlation structure amongst the eight local directed closure coefficients, where coefficients within one block are positively (but not perfectly) correlated while coefficients from distinct blocks are nearly uncorrelated. The block separation coincides with the direction of the closing edge in the closure coefficients. We provide theoretical justification for this observation, gleaned from studying the expected behavior of the closure coefficients for directed configuration model random graphs. Specifically, we show that the expected value (under this model) of each local directed closure coefficient increases with the node degree in the closing edge direction, and thus coefficients with the same closure direction and directed degree are correlated.

From empirical network measurements, we find surprising asymmetry amongst average closure coefficients. Consider the in-out wedges in Fig. 1, where the coefficients  $H_{io}^i(u)$  and  $H_{io}^o(u)$  correspond to the same directed induced subgraph. For such symmetric wedges, the likelihood for outbound closure can be substantially higher than for inbound, even though the two induced subgraphs are structurally identical. On the other hand, we also observe that networks from the same domain exhibit the same asymmetries.

With extremal analysis, we show there is in fact no lower or upper bound on the ratio between types of directed average closure coefficients. Additional analysis under the configuration model shows that the expected value of the directed closure coefficients depend on varied second-order moments of the joint in- and out-degree distribution of the network. This result partly explains the significant difference in values between a pair of seemingly related

average closure coefficients: their expected behaviors correspond to different second order moments of the degree distribution.

Beyond our intrinsic study on the structure of directed closure coefficients, we show that these coefficients can be powerful features for network-based machine learning. In a lawyer advisory network [22] where every node (lawyer) is labeled with a status level (partner or associate) and directed edges correspond to who talks to whom for profession advice, we show that local directed closure coefficients are much better predictors of status compared to other structural features such as degree and directed clustering coefficients [9]. Analysis of the regularization path of the predictive model yields the insight that it is not *how many one advises* but rather *who one advises* that is predictive of partner status. We conduct a similar network classification task in an entirely different domain using a food web from an ecological study. Using the same tools, we find that directed closure coefficients are good predictors of whether or not a species is a fish. This highlights that our proposed measurements are useful across domains.

In summary, we propose the directed closure coefficients, a family of new metrics for directed triadic closure on directed networks. We provide extensive theoretical analysis which help explain some counter-intuitive empirical observations on real-world networks. Through a case study, we also demonstrate that our proposed measurements are good predictors in network-based machine learning tasks.

## 2 BACKGROUND AND PRELIMINARIES

An undirected network (graph)  $G = (V, E)$  is a node set  $V$  and an edge set  $E$ , where an edge  $e \in E$  connects two nodes  $u$  and  $v$ . We use  $d(u)$  to denote the degree of node  $u \in V$ , i.e., the number of edges adjacent to  $u$ . A *wedge* is an ordered pair of edges that share exactly one node; the shared node is the *center* of the wedge. A wedge is *closed* if there is an edge connecting the two non-center nodes (i.e., the nodes in the wedge induce a triangle in the graph).

Perhaps the most common metric for measuring triadic closure in undirected networks is the average clustering coefficient [46]. This metric is the mean of the set of *local clustering coefficients* of the nodes, where the local clustering coefficient of a node  $u$ ,  $C(u)$ , is the fraction of wedges centered at node  $u$  that are closed:

$$C(u) = \frac{2T(u)}{d(u) \cdot (d(u) - 1)},$$

where  $T(u)$  denotes the number of triangles in which node  $u$  participates. The denominator  $d(u) \cdot (d(u) - 1)$  is the number of wedges centered at  $u$ , and the coefficient 2 corresponds to the two wedges (two ordered pairs of neighbors) centered at  $u$  that the triangle closes. If there is no wedge centered at  $u$  (i.e.,  $d(u) \leq 1$ ), the local clustering coefficient is undefined.

Again, to measure the overall triadic closure of the entire network, the *average clustering coefficient* is defined as the mean of the local clustering coefficients of all nodes:  $\frac{1}{|V|} \sum_{u \in V} C(u)$ . When undefined, the local clustering coefficient is treated as zero in this average [34], although there are other ways to handle these cases [20]. An alternative global version of the clustering coefficient is the *global clustering coefficient*, which is the fraction of closed wedges

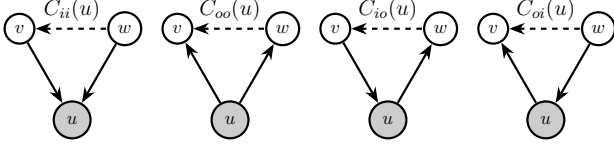


**Figure 2: Illustration of the local directed clustering coefficients at node  $u$ , due to Fagiolo [9]. The definition is a direct extension of the local clustering coefficient [46], which measures triadic closure from the center of each wedge.**

in the entire network [33, 45],

$$C = \frac{2 \sum_{u \in V} T(u)}{\sum_{u \in V} d(u) \cdot (d(u) - 1)}.$$

This measure is also sometimes called *transitivity* [5].

Recent research has exposed fundamental differences in how triadic closure is interpreted and measured [48]. For example, social network triadic closure is often explained by the old adage that “a friend of a friend is my friend,” which accredits the creation of the third edge to the end-node (also called the *head*) of the wedge. This interpretation, however, is fundamentally at odds with how triadic closure is measured by the clustering coefficient, which is from the perspective of the center node. To close this gap, Yin et al. proposed the *local closure coefficient* that measures triadic closure from the head node of wedges. Formally, they define this as  $H(u) = 2T(u)/\sum_{v \in N(u)} [d(v) - 1]$ , where  $N(u)$  is the set of neighbors of  $u$ . In this case, the denominator is the number of length-2 paths emanating from node  $u$ . Thus, in social networks, the closure coefficient of a node  $u$  can be interpreted as the fraction of friends of friends of  $u$  that are themselves friends with  $u$ .

**Extensions to directed networks.** The focus of this paper is on measuring triadic closure in directed networks. The only definitional difference from undirected networks is that the edges are equipped with an orientation, and  $(u, v) \in E$  denotes a directed edge pointing from  $u$  to  $v$ . We assume that  $G$  does not contain multi-edges or self-loops and denote the number of nodes by  $n = |V|$  and the number of edges by  $m = |E|$ .

When an end-node  $u$  of an edge is specified, we denote the direction of an edge as  $i$  (for incoming to  $u$ ) or  $o$  (for outgoing from  $u$ ). For any node  $u \in V$ , we use  $d_i(u)$  and  $d_o(u)$  to denote its *in-degree* and *out-degree*, i.e., the number of edges incoming to and outgoing from node  $u$ , respectively. For a degree sequence  $[d_i(u), d_o(u)]_{u \in V}$ , we use  $M_{xy}$ , with  $x, y \in \{i, o\}$  being the direction indicator, to denote the second-order moments of the degree sequence, i.e.,

$$M_{xy} = \frac{1}{|V|} \sum_{u \in V} d_x(u) d_y(u).$$

There are three second-order moments:  $M_{ii}$ ,  $M_{oo}$ , and  $M_{io} = M_{oi}$ .

Fagiolo proposed a generalization of the clustering coefficient to directed networks [9]. Similar to the undirected case, a *directed wedge* is an *ordered* pair of edges that share a common node, and the common node is called the *center* of this wedge. The wedge is then called *closed* if there is an edge from the opposite end-point of the first edge to the opposite end-point of the second edge (this constraint, along with the ordering of the two edges, covers the symmetries in the problem). In total, there are four directed clustering coefficients, each defined by the fraction of certain types of wedges that are closed (Figure 2). Seshadhri et al. extended the

Fagiolo definition by explicitly accounting for bi-directed edges [43], with a focus on network-level (as opposed to node-level) metrics. While we could also explicitly differentiate bi-directed links, here we focus on bi-directed links as counting towards closure in both directions.

Directed clustering coefficients have found applications in analyzing fMRI data [26], financial relationships [30], and social networks [1]. However, as discussed above, existing directed clustering coefficients measure clustering from the center of a wedge, a limited perspective. Our head-based directed closure coefficients thus enhance the toolkit for these diverse applications studying clustering in directed networks.

**Additional related work.** The first research on directed triadic closure is due to Davis and Leinhardt [8] who studied the relative frequency of each 3-node directed subgraph pattern and compared the frequencies with random graph models. Milo et al. later examined significantly recurring patterns of connected directed subgraphs as “network motifs” [29], with a particular emphasis on the role of so-called “feed-forward loops” in biology [28]. Similar to the case of directed clustering coefficients [9], prior research has studied the ratio of closed wedges at the global (network) level [6, 35, 43], which is sometimes called “motif intensity” [35]. The key differences in our definitions are that (i) we measure closure at the node level and (ii) it is a head-node-based metric which agree with our intuition as driven by traditional explanation in directed triadic closure. We find that our measures have considerably different behavior than previous measures.

Directed triad closure also appears in dynamic network analysis. Lou et al. proposed a graphical model to predict the formation of a certain type of directed triadic closure: closing an *oo*-type wedge with outbound link [27]. This model was later generalized to predict the closure of any type of wedge based on node attributes [18]. Similarly, the notion of a “closure ratio” has been used to analyze copying phenomena [41]. This is also an end-node-based metric that measures a temporal closure of in-in wedges with an incoming edge. Our definitions of directed closure coefficients are different in that they (i) are defined on static networks, (ii) study diverse types of triadic closure, and (iii) are closely connected to undirected measures of closure and the traditional perspective of triadic closure. Connecting our static measures of directed closure and temporal counterparts is an interesting problem beyond the scope of this work.

### 3 DIRECTED CLOSURE COEFFICIENTS

In this section, we provide our formal definition of directed closure coefficients, and measure them on some representative real-world networks to demonstrate how they provide empirical insights. These insights provide direction and motivation for our theoretical analysis in Section 4. We later show how directed closure coefficients are useful features in machine learning tasks in Section 5.

**Definitions.** With the same motivation as the undirected closure coefficient, we propose to measure directed triadic closure from the endpoint of a directed wedge. Recall that a directed wedge is an ordered pair of edges that share exactly one common node. The common node is called the center of the wedge, and here we define the *head* of this wedge as the other end of the first edge, and the

tail as the other end of the second edge. Regardless of the direction of the edges, we denote a wedge by a node triple  $(u, v, w)$ , where  $u$  is the head,  $v$  is the center, and  $w$  is the tail.

Since each edge is directed, there are four types of directed wedges.<sup>1</sup> We denote the type of wedge with two variables, say  $x$  and  $y$ , each taking a value in  $\{i, o\}$  to denote incoming or outgoing. Specifically, a wedge is of type  $xy$  (an  $xy$ -wedge) if the first edge is of direction  $x$  to the head, and the second edge is of direction  $y$  to the center node. Figure 1 shows the four types of directed wedges.

We say that a wedge is  $i$ -closed if there is an incoming edge from the tail to the head node, and analogously, it is  $o$ -closed if there is an outgoing edge from head to the tail node. For any  $u \in V$  and  $x, y, z \in \{i, o\}$ , we denote  $W_{xy}(u)$  as the number of wedges of type  $xy$  where node  $u$  is the head, and  $T_{xy}^z(u)$  as the number of  $z$ -closed wedges of type  $xy$  where node  $u$  is the head.

Now we give our formal definition of local directed closure coefficients, which is also illustrated in Figure 1.

**Definition 3.1.** The **local directed closure coefficients** of node  $u$  are eight scalars, denoted by  $H_{xy}^z(u)$  with  $x, y, z \in \{i, o\}$ , where

$$H_{xy}^z(u) = \frac{T_{xy}^z(u)}{W_{xy}(u)}. \quad (1)$$

If there is no wedge of certain type with node  $u$  being the head, the corresponding two closure coefficients are undefined.

Here we highlight again the fundamental difference between the local directed closure coefficients we proposed and the local directed clustering coefficients proposed by Fagiolo [9]: the closure coefficients measure clustering from the head of wedges, which agrees with natural initiator-driven explanations on triadic closure, while the clustering coefficients measure from the center of wedges. We will show that this small definitional difference yields substantial empirical and theoretical disparity.

Analogous to the undirected clustering coefficient, we also define the average and global directed closure coefficient to measure the overall directed triadic closure tendency of the network.

**Definition 3.2.** The **average directed closure coefficients** of a graph are eight scalars, denoted by  $\bar{H}_{xy}^z$  with  $x, y, z \in \{i, o\}$ , each being the mean of corresponding local directed closure coefficient across the network:

$$\bar{H}_{xy}^z = \frac{1}{n} \sum_{u \in V} H_{xy}^z(u),$$

We treat local closure coefficients that are undefined as taking the value 0 in this average, though most nodes in the datasets we analyze have eight well-defined closure coefficients.

**Definition 3.3.** The **global directed closure coefficients** of a graph are eight scalars, denoted by  $H_{xy}^z$  with  $x, y, z \in \{i, o\}$ , each being the fraction of closed directed wedges in the entire network:

$$H_{xy}^z = \frac{T_{xy}^z}{W_{xy}}, \quad (2)$$

where  $W_{xy} = \sum_{u \in V} W_{xy}(u)$  and  $T_{xy}^z = \sum_{u \in V} T_{xy}^z(u)$  are the total number of  $xy$ -wedges and closed  $xy$ -wedges.

<sup>1</sup>For readability purposes, we do not consider reciprocated edges [43] separately in this paper, but treat each reciprocated edge as two independent directed edges. Our definitions and analyses are easily extended to study reciprocated edges, where there would be 9 types of directed wedges and 27 closure coefficients.

**Table 1: Summary statistics of networks: the number of nodes  $n$ , number of edges  $m$ , and the second-order moments of the degree sequence  $M_{ii}$ ,  $M_{io}$ , and  $M_{oo}$ .**

Network	$n$	$m$	$M_{ii}$	$M_{io}$	$M_{oo}$
SOC-LAWYER	71	892	227.41	166.15	208.65
SOC-EPINIONS	75.9K	509K	1179.40	526.15	721.82
SOC-LIVEJOURNAL	4.85M	69.0M	2091.52	1220.33	1504.35
MSG-COLLEGE	1899	20.3K	347.80	391.99	592.42
EMAIL-EU	1005	25.6K	1428.97	1509.56	1756.77
CIT-HEPTh	27.8K	353K	1746.72	269.14	416.35
CIT-HEPPh	34.5K	422K	790.63	189.62	380.70
FW-EVERGLADES	69	916	394.12	136.52	257.16
FW-FLORIDA	128	2106	493.08	201.92	451.62
WEB-GOOGLE	876K	5.11M	1572.90	69.30	77.46
WEB-BERKSTAN	685K	7.60M	62430.80	324.71	390.55

The global directed closure coefficients are equivalent to some global metrics of directed clustering coefficients [35, 43], since the difference in measuring from head or center does not surface.

**Empirical analysis.** To obtain intuitions and empirical insights before diving into theoretical analysis, we evaluate the directed closure coefficients on 11 networks from five different domains:

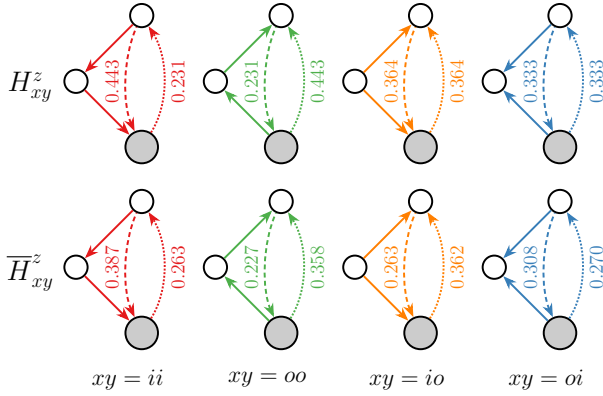
- Three social networks. SOC-LAWYER: a professional advisory network between lawyers in a law firm [22]; SOC-EPINIONS [39] and SOC-LIVEJOURNAL [2]: two online friendship networks.
- Two communication networks. MSG-COLLEGE [36]: a message network between college students; EMAIL-EU [49]: an email network between researchers at a European institute.
- Two citation networks. CIT-HEPTh and CIT-HEPPh [13]: constructed from arXiv submission in two categories.
- Two food webs. FW-FLORIDA [44] collected from the Florida Bay and FW-EVERGLADES [44] from the Everglades Wetland.
- Two web graphs. WEB-GOOGLE [25] from Google and WEB-BERKSTAN [25] from berkely.edu and stanford.edu domains.

Table 1 provides basic statistics of the networks.

Figure 3 shows the global and average directed closure coefficients of the SOC-LAWYER dataset. From the first row, we see that the eight global closure coefficients can be grouped into four pairs,

$$\{(H_{ii}^i, H_{oo}^o), (H_{ii}^o, H_{oo}^i), (H_{io}^i, H_{io}^o), (H_{oi}^i, H_{oi}^o)\}$$

with each pair of coefficients taking the same value. This observation is expected due to the symmetry in the wedge structure, which we explore in more detail in Section 4.1. In contrast, these groupings do not take the same value in the case of the average closure coefficients (the second row of Figure 3): we observe an *a priori* unexpected asymmetry. For example,  $\bar{H}_{io}^o = 0.362 \gg \bar{H}_{io}^i = 0.263$  (in orange, Fig. 3). When an in-out wedge is closed with either an incoming or outgoing edge, the induced triangle is actually the same: both are feedforward loops [29]. It is not obvious why the closure with an outgoing edge is so much more likely than with an incoming edge. We develop some theoretical explanations for this asymmetry in Section 4.2.



**Figure 3: Global (top) and average (bottom) directed closure coefficients in soc-LAWYER, with head nodes highlighted in gray. The global closure coefficients exhibit symmetry (e.g.,  $H_{io}^i = H_{io}^o$ ), while the average closure coefficients exhibit counter-intuitive asymmetry between pairs of coefficients, e.g.,  $\bar{H}_{io}^i = 0.263 \ll \bar{H}_{io}^o = 0.362$  (in orange, second row). The induced structure is the same in both closure coefficients (a feedforward loop). We explain this phenomenon in Section 4.**

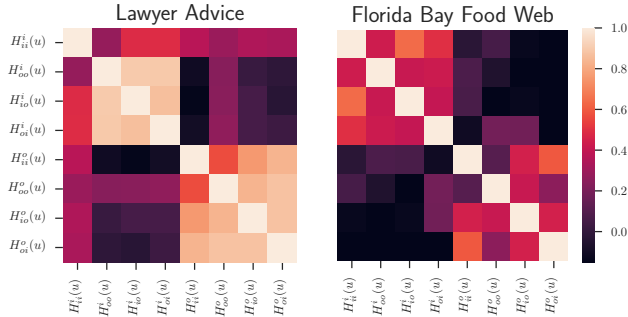


**Figure 4: Heatmap of the correlation matrix of the eight local directed closure coefficients in soc-LAWYER (left) and FW-FLORIDA (right). There is a clear separation on the eight local closure coefficients: the ones for  $i$ -closed and the ones for  $o$ -closed. Coefficients within each group are highly correlated while between groups are almost uncorrelated.**

We also explore the correlations between the eight average directed closure coefficients in the soc-LAWYER and FW-FLORIDA networks (Fig. 4). Each network has a clear separation amongst the eight local closure coefficients: the coefficients in the first four rows/columns (with incoming closure edge), and the coefficients on the last four rows/columns (with outgoing closure edge). Within each group, the coefficients are strongly correlated. In soc-LAWYER, the coefficients in different groups are nearly uncorrelated, whereas in FW-FLORIDA, the coefficients in different groups are negatively correlated. This correlation pattern is representative across the networks that we have studied with directed closure coefficients, and we explain this correlation separation as part of the next section.

To study the difference in frequencies of directed triadic closure, we visualize the eight average directed closure coefficients of 10 networks in Figure 5, where each row contains two networks within the same domain. We find that each domain of networks has their

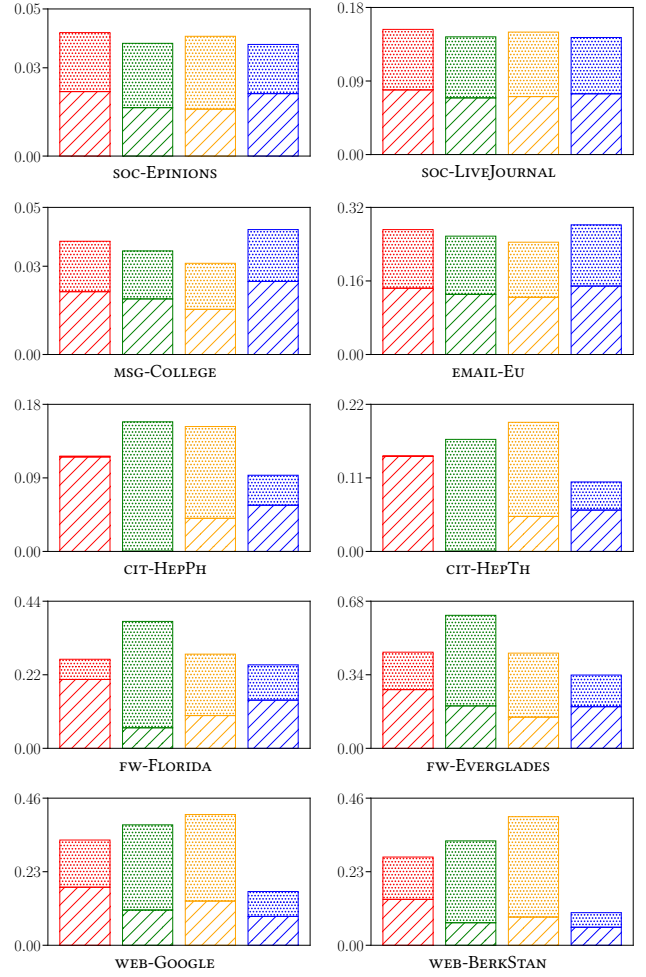


**Figure 5: Average directed closure coefficients of networks from five domains. Wedge types are colored in the same way as in Figure 3, with incoming closure represented by slashed-bars and outgoing closure represented by dotted-bars. Networks from the same domain (each row) have similar directed closure patterns, while the patterns across domains can be highly different.**

own directed triadic closure patterns. In social networks, different wedge types have similar closure frequencies, which is due to the abundance of reciprocated edges [32]. In communication networks, the tall blue bars associated with out-in wedge type means one is more likely to connect to people with whom they both send communications; this might be a result of shared interest. In contrast, citation networks have low closure coefficients for out-in wedge (short blue bars), meaning that one is not likely to cite or be cited by papers with the same reference: this phenomenon might come from a conflict of interest; moreover, due to near non-existence of cycles, in-in wedges and out-out wedges are each only closed in one direction. Similar patterns appear in the food webs and web graphs, where there is a hierarchical structure and a lack of cycles. Lastly, we observe similar asymmetry in all citation, food web, and

web graphs,  $\bar{H}_{io}^o \geq \bar{H}_{io}^i$ , from the orange bars showing significantly higher outbound closure rate than inbound rate.

## 4 THEORETICAL ANALYSIS

We now provide theoretical analysis of our directed closure coefficients. We first show the symmetry between the four pairs of global directed closure coefficients. Motivated by the empirical asymmetry amongst average directed closure coefficients, we prove that this asymmetry can be unboundedly large. Finally, to explain the asymmetry, we study how the degree distribution influences the expected value of each average closure coefficients under a directed configuration model with a fixed joint degree distribution.

### 4.1 Symmetry and Asymmetry

Recall that each global directed closure coefficient is the fraction of certain type of closed wedges in the entire network. We observed in Section 3 that the eight global directed closure coefficients can be grouped into four pairs, with each pair of coefficients having the same value. We now justify this result in the following proposition, which says that these values must be the same in any network.

**PROPOSITION 4.1.** *In any directed network, we have  $H_{ii}^i = H_{oo}^o$ ,  $H_{ii}^o = H_{oo}^i$ ,  $H_{io}^i = H_{io}^o$ , and  $H_{oi}^i = H_{oi}^o$ .*

**PROOF.** Here we only prove  $H_{ii}^i = H_{oo}^o$ , and the other three identities can be shown analogously. By counting wedges from the center node,  $W_{ii} = \sum_u d_i(u) \cdot d_o(u) = W_{oo}$ . Next, there is a one-to-one correspondence between a closed in-in wedge and a closed out-out wedge by flipping the roles of the head and tail nodes. Thus,  $T_{ii}^i = T_{oo}^o$  and  $H_{ii}^i = H_{oo}^o$ , according to Definition 3.3.  $\square$

Proposition 4.1 illustrates the fundamental symmetry among the eight global directed closure coefficients. The four pairs of global closure coefficients  $\{(H_{ii}^i, H_{oo}^o), (H_{ii}^o, H_{oo}^i), (H_{io}^i, H_{io}^o), (H_{oi}^i, H_{oi}^o)\}$  correspond to the same structure and triadic closure pattern in the entire network, so their values have to be the same.





As an alternative global measure of directed triadic closure, we might expect the average closure coefficients to have the similar symmetric pattern. Specifically, by pairing up the average closure coefficients in the same way,

$$\{(\bar{H}_{ii}^i, \bar{H}_{oo}^o), (\bar{H}_{ii}^o, \bar{H}_{oo}^i), (\bar{H}_{io}^i, \bar{H}_{io}^o), (\bar{H}_{oi}^i, \bar{H}_{oi}^o)\}, \quad (3)$$

one might initially guess that the two values in a pair would be close. However, our empirical evaluation on the soc-LAWYER datasets above, as well as all the citation, food webs, and web graphs, showed *asymmetry* in these metrics, specifically  $\bar{H}_{io}^o \gg \bar{H}_{io}^i$ . Here we study how large can such difference be and find that there is no trivial upper or lower bound on  $\bar{H}_{io}^i$  based on  $\bar{H}_{io}^o$  and vice versa. Furthermore, this same flavor of unboundedness is valid for the other three pairs of average directed closure coefficients.

**THEOREM 4.2.** *For any  $\epsilon > 0$ , and any pair of average directed closure coefficients from Equation (3), denoted as  $(\bar{H}_a, \bar{H}_b)$ , there is a finite graph such that  $\bar{H}_a < \epsilon$  and  $\bar{H}_b > 1 - \epsilon$ , and another finite graph such that  $\bar{H}_a > 1 - \epsilon$  and  $\bar{H}_b < \epsilon$ .*

**PROOF.** Here we give a constructive proof for the pair  $(\bar{H}_{io}^i, \bar{H}_{io}^o)$ ; the same technique works for the other three pairs. We use the

Class	#nodes	$W_{io}(u)$	$T_{io}^i(u)$	$T_{io}^o(u)$
	$n_1$	$n_3 n_2 + n_3 n_4$	$n_3 n_2$	0
	$n_2$	$n_3 n_1 + n_3 n_4$	0	$n_3 n_1$
	$n_3$	0	0	0
	$n_4$	$n_3 n_1 + n_3 n_2$	0	0

**Figure 6: An example graph used in the proof of Theorem 4.2, showing maximal differences between directed closure coefficients  $\bar{H}_{io}^i$  and  $\bar{H}_{io}^o$ . Each double circle  $C_j$  represents a class of nodes and an edge  $C_j \rightarrow C_k$  means that  $u_j \rightarrow u_k$  for all  $u_j \in C_j$  and  $u_k \in C_k$ .**

example graph in Figure 6. Each double-circle in the figure, denoted by  $C_j$  with  $j \in \{1, 2, 3, 4\}$ , represents a set of nodes, and we let  $n_j$  denote the number of nodes in each class. A directed edge from class  $C_j$  to  $C_k$  means that for any node  $u_j \in C_j$  and any node  $u_k \in C_k$ , there is an edge  $u_j \rightarrow u_k$ . The number of in-out wedges as well as closed wedges are listed in the last three columns of the table. We have that  $H_{io}^i(u) = \frac{n_2}{n_2 + n_4}$  for any node  $u \in C_1$ ,  $H_{io}^i(u) = 0$  for  $u \in C_2$  or  $C_4$ , and  $H_{io}^i(u)$  undefined for  $u \in C_3$ . Now,

$$\bar{H}_{io}^i = \frac{n_1 n_2}{(n_2 + n_4)(n_1 + n_2 + n_3 + n_4)}, \quad \bar{H}_{io}^o = \frac{n_1 n_2}{(n_1 + n_4)(n_1 + n_2 + n_3 + n_4)}.$$

The  $n_j$ 's can take any integer value. We first fix  $n_3 = n_4 = 1$ . If  $n_1 = k^2$  and  $n_2 = k$  for any integer  $k > 3/\epsilon$ ,  $\bar{H}_{io}^i > 1 - \epsilon$  and  $\bar{H}_{io}^o < \epsilon$ . And if  $n_1 = k$  and  $n_2 = k^2$  for any integer  $k > 3/\epsilon$ , one can verify that  $\bar{H}_{io}^i < \epsilon$  and  $\bar{H}_{io}^o > 1 - \epsilon$ .  $\square$

In contrast, since the directed clustering coefficients due to Fagiolo [9] are based on the center of wedges, the two edges are naturally symmetric, and consequently the metric is always symmetric. Therefore, the directed clustering coefficients have only four dimensions while our directed closure coefficients have eight.

In the next section, we study how we expect the directed closure coefficients to behave in a configuration model, which provides additional insight into why asymmetries in the directed closure coefficients might be unsurprising.

### 4.2 Expectations under configuration

The previous section showed that pairs of average directed closure coefficients can have significantly different values; in fact, our extremal analysis showed that their ratio is in fact unbounded in theory. However, we have not yet provided any intuition for asymmetry in real-world networks. Here, we provide further theoretical analysis to show that the structure of the joint in- and out-degree distribution of a network provides one explanation of this asymmetry. When considering random graphs generated under a directed configuration model with a fixed joint degree sequence, the coefficients are generally asymmetric even in their expectations.

The configuration model [11, 31] is a standard tool for analyzing the behavior of patterns and measures on networks. The model

is typically studied for undirected graphs with a specified degree sequence, but the idea cleanly generalizes to directed graphs with a specified joint degree sequence [7]. It is often hard to understand the determinants of unintuitive observations on networks. What aspect of the specific network under examination leads to a given observation? As one specific angle on this question, does the observation hold for typical graphs with the observed joint degree sequence, and if so, what are the determinants of the behavior? Analyses using the configuration model can thus be used to investigate the expected behavior of a measure, in our case the directed closure coefficients, under this random graph distribution.

An important property of the configuration model is that, for degree sequences that correspond to sparse graphs, the probability of forming an edge  $u \rightarrow v$  is of the order of  $d_o(u) \cdot d_i(v)/m$ , where  $m$  is the total number of edges [34]. As further notation for this section, for an event denoted by  $A$ , we use  $1_{[A]}$  as the indicator function for event  $A$ , i.e.,  $1_{[A]} = 1$  when event  $A$  happens and 0 otherwise. For any direction variable  $x \in \{i, o\}$ , we use  $\bar{x}$  to denote the opposite direction of  $x$ . Now we have the following theoretical results on the expected value of local directed closure coefficients under the directed configuration model, which relates the expected closure coefficient of node  $u$  with closing direction  $i$  and  $o$  to the in- and out-degrees  $d_i(u)$  and  $d_o(u)$  of  $u$ .

**THEOREM 4.3.** *Let  $S$  be a joint degree sequence and  $G$  a random directed graph sampled from the directed configuration model with  $S$ . For any node  $u$  and any local directed closure coefficient  $H_{xy}^z(u)$ ,*

$$\mathbb{E}[H_{xy}^z(u)|S] = \frac{n(d_z(u) - 1_{[x=z]})}{m^2} \cdot \left( M_{\bar{y}\bar{z}} - 1_{[y=z]} \cdot \frac{m}{n} \right) \cdot (1 + o(1)),$$

where  $M_{\bar{y}\bar{z}}$  is the second-order moment of degree sequence  $S$ .

**PROOF.** For any wedge  $(u, v, w)$  of type  $xy$  whose head is  $u$ , this wedge is  $z$ -closed if there is an edge between  $u$  and  $w$  of direction  $z$  (with respect to  $u$ ). A  $z$ -closed wedge occurs if we match a  $z$ -stub from node  $u$  and a  $\bar{z}$ -stub from node  $w$ . Note that the number of  $z$ -stubs of node  $u$  that are not used in wedge  $(u, v, w)$  is  $(d_z(u) - 1_{[x=z]})$ , where we need to subtract the indicator function because one  $z$ -stub is already used in wedge  $(u, v, w)$  if  $x = z$ . Similarly, the number of  $\bar{z}$ -stubs of node  $w$  that are not used in wedge  $(u, v, w)$  is  $(d_{\bar{z}}(w) - 1_{[\bar{y}=\bar{z}]})$ . Note that  $H_{xy}^z(u)$  can be directly interpreted as the probability that a random wedge  $(u, v, w)$  is  $z$ -closed. According to the setup of directed configuration model, this probability is on the order of

$$(d_z(u) - 1_{[x=z]}) \cdot (d_{\bar{z}}(w) - 1_{[\bar{y}=\bar{z}]})/m.$$

Therefore,

$$\begin{aligned} \mathbb{E}[H_{xy}^z(u)|S] &\sim \mathbb{E}[(d_z(u) - 1_{[x=z]}) \cdot (d_{\bar{z}}(w) - 1_{[\bar{y}=\bar{z}]})/m] \\ &= \frac{d_z(u) - 1_{[x=z]}}{m} \cdot \left( \mathbb{E}[d_{\bar{z}}(w)|S] - 1_{[\bar{y}=\bar{z}]} \right), \end{aligned} \quad (4)$$

where the second step follows from the fact that the only random variable is the degree of a random tail node  $w$ .

Now we show that  $\mathbb{E}[d_{\bar{z}}(w)|S] = n/m \cdot M_{\bar{y}\bar{z}}$ . Note that  $w$  is not a uniformly random node, it is the tail node of a random wedge whose head is  $u$ . In the directed configuration model where edges are created from random stub matching, the probability that a node  $w$  is the tail of a  $xy$ -wedge is the same probability that  $w$  is the

endpoint of a random edge and the direction of the edge to  $w$  is  $\bar{y}$ . Therefore, the probability that any node  $w$  is the tail of the wedge is proportional to  $d_{\bar{y}}(w)$ . Now since  $\sum_{w \in V} d_{\bar{y}}(w) = m$ , we have

$$\mathbb{E}[d_{\bar{z}}(w)|S] = \sum_{w \in V} \frac{d_{\bar{y}}(w)}{m} \cdot d_{\bar{z}}(w) = \frac{n}{m} \cdot M_{\bar{y}\bar{z}}. \quad (5)$$

Combining Equations (4) and (5) completes the proof.  $\square$

Theorem 4.3 shows that the expected value of the local directed closure coefficient  $H_{xy}^z(u)$  increases with  $d_z(u)$ , the degree in the direction of closure. One corollary of this result is that under the configuration model the expected values of the local closure coefficient with the same closure direction are all monotonic with the same corresponding degree, and thus they should be correlated themselves. This result provides one intuition for the block structure of the correlations between coefficients found in Figure 4.

We can easily aggregate the results of Theorem 4.3 to give expected values of the average directed closure coefficients.

**THEOREM 4.4.** *Let  $S$  be a joint degree sequence and  $G$  be a random directed graph generated from the directed configuration model with  $S$ . For any average directed closure coefficient  $\bar{H}_{xy}^z$ ,*

$$\mathbb{E}[\bar{H}_{xy}^z|S] = \frac{m - n \cdot 1_{[x=z]}}{m^2} \cdot \left( M_{\bar{y}\bar{z}} - 1_{[y=z]} \cdot \frac{m}{n} \right) \cdot (1 + o(1)).$$

**PROOF.** We have

$$\begin{aligned} \mathbb{E}[\bar{H}_{xy}^z|S] &= \frac{1}{n} \sum_u \mathbb{E}[H_{xy}^z(u)|S] \\ &\sim \left( M_{\bar{y}\bar{z}} - 1_{[y=z]} \cdot \frac{m}{n} \right) \cdot \frac{1}{m^2} \sum_u [d_z(u) - 1_{[x=z]}] \\ &= \left( M_{\bar{y}\bar{z}} - 1_{[y=z]} \cdot \frac{m}{n} \right) \cdot \frac{m - n \cdot 1_{[x=z]}}{m^2}, \end{aligned}$$

where the first line is due to Theorem 4.3.  $\square$

Theorem 4.4 shows that the expected value of any average closure coefficient  $\bar{H}_{xy}^z$  is mainly determined by  $M_{\bar{y}\bar{z}}$ , a second-order moment of the degree sequence. In the soc-LAWYER dataset, we have  $M_{io} = 166.15 \ll 227.41 = M_{ii}$ , meaning that  $\mathbb{E}[\bar{H}_{io}^i] \ll \mathbb{E}[\bar{H}_{io}^o]$ . This result (partly) explains the asymmetry observed in Figure 3: the different coefficients are related to different moments of the joint degree sequence of the network, at least for graphs sampled from a configuration model with different empirical joint degree sequences.

Finally, we can also determine the expected value of global directed closure coefficients.

**THEOREM 4.5.** *Let  $S$  be a joint degree sequence and  $G$  be a random directed graph generated from the directed configuration model with  $S$ . For any global directed closure coefficient  $H_{xy}^z$ ,*

$$\mathbb{E}[H_{xy}^z|S] = \left( M_{\bar{y}\bar{z}} - 1_{[y=z]} \cdot \frac{m}{n} \right) \cdot \left( M_{xz} - 1_{[x=z]} \cdot \frac{m}{n} \right) \cdot \frac{n^2}{m^3} \cdot (1 + o(1)).$$

**PROOF.** For a random type- $xy$  wedge  $(u, v, w)$ , we have shown that the probability of it being  $z$ -closed is of the order  $(d_z(u) - 1_{[x=z]}) \cdot (d_{\bar{z}}(w) - 1_{[\bar{y}=\bar{z}]})/m$ , so



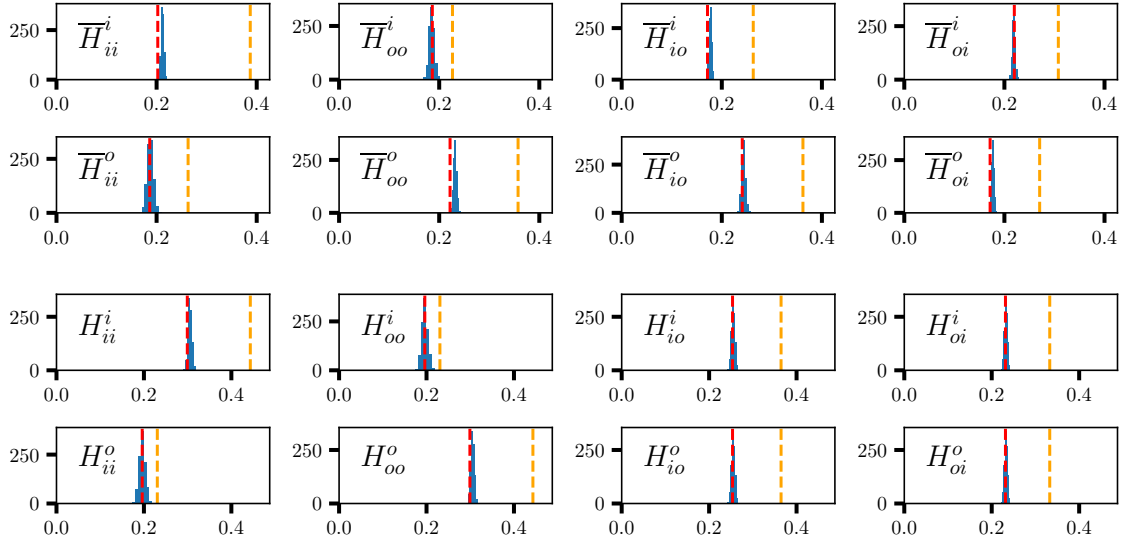


**Figure 7: Histogram of each average closure coefficient (first two rows) and global closure coefficient (last two rows) in 1,000 directed configuration model random graphs with the joint degree sequence of the soc-LAWYER network. The  $x$ -axis is the value of various directed closure coefficients and the  $y$ -axis is the frequency. Besides the histogram, we also plot the expected value of closure coefficients from Theorems 4.4 and 4.5 (red) as well as the actual value in the original network (orange).**

$$\begin{aligned} \mathbb{E}[H_{xy}^z | S] &\sim \frac{1}{m} \cdot \mathbb{E}[(d_z(u) - \mathbf{1}_{[x=z]}) \cdot (d_z(w) - \mathbf{1}_{[\bar{y}=\bar{z}]}) | S] \\ &\sim \frac{1}{m} \cdot \left( \mathbb{E}[d_z(u) | S] - \mathbf{1}_{[x=z]} \right) \cdot \left( \mathbb{E}[d_z(w) | S] - \mathbf{1}_{[\bar{y}=\bar{z}]} \right). \end{aligned}$$

The first line is different from Equation (4) in that here we consider all the wedges in the network, instead of only those whose head is  $u$ . Consequently we also need to take the expectation over the choice of node  $u$ . The second line follows from the fact that the choice of node  $u$  and  $w$  are approximately independent in the configuration model. Equivalent to Equation (5),  $\mathbb{E}[d_z(w) | S] = \frac{n}{m} \cdot M_{\bar{y}\bar{z}}$  and  $\mathbb{E}[d_z(u) | S] = \frac{n}{m} \cdot M_{xz}$ . Combining these completes the proof.  $\square$

Simulations that sample from the configuration model show a tight concentration of the coefficients around the asymptotic expected values we derive here. Implementational details and results are given in supplementary material.

As a byproduct of our analysis, the proof of Theorem 4.5 also shows that, under the directed configuration model, the probability that a wedge is closed is independent of the center node, and thus equal to the network-level average. This observation gives us the expected value of Fagiolo’s directed local clustering coefficients [9] under this random graph model as well.

**PROPOSITION 4.6.** *Let  $S$  be a joint degree sequence and  $G$  be a random directed graph generated from the directed configuration model with  $S$ . For local directed clustering coefficient  $C_{xy}(u)$ ,*

$$\mathbb{E}[C_{xy}(u) | S] = \mathbb{E}[H_{\bar{x}\bar{y}}^i | S].$$

**PROOF.** Consider a random wedge with  $u$  being the center node,  $(v, u, w)$ , which is an  $\bar{x}\bar{y}$ -wedge to node  $v$ . From the definition of  $C_{xy}(u)$ , this wedge is closed if it is  $i$ -closed to node  $v$ . Since the probability of this wedge being  $i$ -closed is independent of node  $u$ , it

is the same as if we randomly choose a wedge without constraining node  $u$  as the center, and thus  $\mathbb{E}[C_{xy}(u) | S] = \mathbb{E}[H_{\bar{x}\bar{y}}^i | S]$ .  $\square$

**Simulations.** We now study the accuracy of the theoretical expected values of the average and global closure coefficients under the directed configuration model.

The directed configuration model can be sampled by using double-edge swaps [37]. To sample graphs from the model, we begin with an empirical graph (the graph of interest) with joint degree sequence  $S$ . We then select a pair of random directed edges to swap, which changes the graph slightly but notably preserves the degree sequence. Taking care to avoid self-loops and multi-edges [11], the double-edge swap can be interpreted as a random walk in the space of simple graphs with the same degree sequence, and the stationary distribution of this random walk is the uniform distribution over the network space. The swap is then repeated many many times to generate graphs that are sampled from the stationary distribution. The mixing time of these random walks are generally believed to be well-behaved, but few rigorous results are known [15].

We generate 1,000 random graphs with the same joint degree sequence as the soc-LAWYER network; to generate each graph we repeat the edge-swapping procedure 10,000 times. Figure 7 exhibits histograms of the distribution of each average and global closure coefficient under this configuration model. We see that our approximate formulas from Theorems 4.4 and 4.5 are very accurate even when the network is only moderate in size ( $n = 71$ ). The theoretical formulas are only guaranteed to be accurate on large sparse networks, and we do observe a small difference between the expected and simulated means (e.g.,  $\bar{H}_{ii}^i$ ).

The simulation shows that the average and global closure coefficients have low variance under this configuration model, and



**Table 2: Validation set accuracy and AUC in classifying node types in the soc-LAWYER dataset (partner vs. associate). Our proposed local directed closure coefficients are the best set of predictors, illustrating the utility of directed closure coefficients in node-level prediction tasks. In contrast, the local directed clustering coefficients [9] are not as effective.**

	degree	closure	closure + degree	clustering	clustering + degree
accuracy	0.7884	<b>0.8743</b>	0.8585	0.6255	0.7884
AUC	0.8763	<b>0.9235</b>	0.9183	0.6362	0.8765

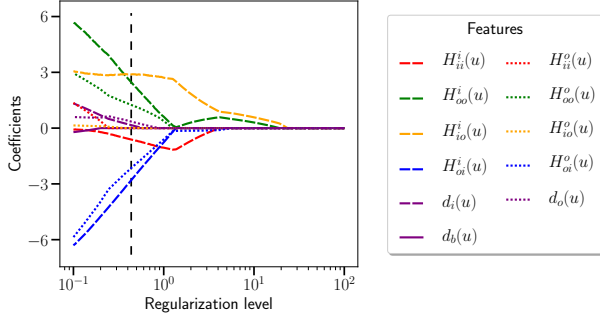


**Figure 8: Regularization path of the  $\ell_1$ -regularized logistic regression model with predictor set closure + degree. The  $x$ -axis is the regularization level, and the  $y$ -axis is the regression coefficient for each predictor. The vertical black dashed line represents the optimal regularization level obtained from cross-validation. The degree attributes are not selected until very low penalization levels, and various local directed closure coefficients dominate the prediction model.**

the values in the original network deviate significantly from these distributions. We interpret this as a further sign that the directed closure coefficients of empirical networks in fact capture empirical structure that is interesting, beyond what one would expect from a graph drawn uniformly at random from the space of graphs with the same joint degree sequence.

## 5 CASE STUDY IN NODE-TYPE PREDICTION

Now that we have a theoretical understanding of our directed closure coefficients, we turn to applications. Directed closure coefficients are a new measurement for directed triadic closure and thus can serve as a feature for network analysis and inference. In this section, we present two illustrative examples to exhibit the strong predictive potential in directed closure coefficients. Specifically, we present two case studies of node-type classification task, where we show the utility of local directed closure coefficients in predicting node type in the soc-LAWYER and FW-FLORIDA dataset analyzed above. By using an interpretable regularized model, we are able to identify the salient directed closure coefficients that are useful for prediction. This analysis reveals new social status patterns in the social network and also automatically identifies previously-studied triadic patterns in food webs as good predictors.

**Table 3: Validation set accuracy and AUC in classifying node types in the fw-FLORIDA dataset (fish vs. non-fish). Our proposed local directed closure coefficients are again the best set of predictors (see also Table 2), illustrating the utility of directed closure coefficients in node-level prediction tasks outside of social network analysis.**

	degree	closure	closure + degree	clustering	clustering + degree
accuracy	0.6250	<b>0.8735</b>	0.8700	0.6875	0.7366
AUC	0.6772	<b>0.9538</b>	0.9529	0.7472	0.7834

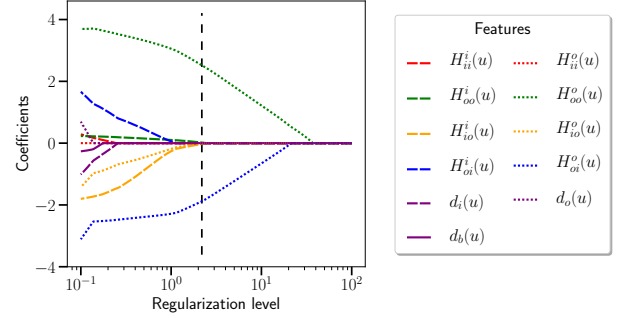


**Figure 9: Regularization path of the  $\ell_1$ -regularized logistic regression model with predictor set closure + degree. The  $x$ -axis is the regularization level, and the  $y$ -axis is the regression coefficient for each predictor. The vertical black dashed line represents the optimal regularization level obtained from cross-validation. The degree attributes are not selected until very low penalization levels, and various local directed closure coefficients dominate the prediction model.**

### 5.1 Case Study I: Classifying node types in a corporate social network

The soc-LAWYER dataset collected by Lazega is a social network of lawyers at a corporate firm [22]. There is a node for each of the 71 lawyers, and each is labeled with a status level—*partner* or *associate*. Of the 71 lawyers in the dataset, 36 are partners and 35 are associates. The edges come from survey responses on who individuals go to for professional advice: there is an edge from  $i$  to  $j$  if person  $i$  went to person  $j$  for professional advice. Of the edges, there are 395 between two partners; 196 between two associates; 59 from partner to associate; and 242 from associate to partner.

In this case study, our goal is to predict the status of the lawyers (associate or partner) with predictors extracted from the advice network. We consider the following five sets of network attributes as predictors:

- (1) **degree**: the in- and out-degree, as well as the number of reciprocal edges at each node;
- (2) **closure**: the eight local directed closure coefficients defined in this paper;
- (3) **closure + degree**: the union of the closure coefficients and the degree predictors;
- (4) **clustering**: the four local directed clustering coefficients as defined by Fagiolo [9]; and
- (5) **clustering + degree**: the union of the local directed clustering coefficients and the degree predictors.

For each predictor set, we use 100 random instances of 3-fold cross-validation to select an  $\ell_1$ -regularized logistic regression model for predicting whether or not a node is a partner (i.e., the positive label is for partner). Table 2 reports validation set accuracy and AUC. The predictors that include our local directed closure coefficients substantially outperform the other predictor sets (an 8% absolute improvement in accuracy and 5% absolute improvement in AUC). The predictor set that includes both degrees and closure coefficients slightly underperforms the one with only closure coefficients, indicating slight overfitting in the training data, which implies that the degree attributes provides redundant and noisy information in addition to the closure coefficient attributes in this prediction task. Note that even though different predictors set have different dimensions, evaluating the performance on the evaluation set makes them comparable.

To understand how the directed local closure coefficients improves prediction performance, we analyze the regularization path of our model [12], a standard method in sparse regression to visualize the predictors at each regularization level. Figure 8 shows the regularization path for the predictor set that includes both the local directed closure coefficients and the degree predictors.

We highlight a few important observations. First, as regularization is decreased, directed local closure coefficients are selected before the degree predictors, indicating that the closure coefficients are more relevant in prediction than degrees. Second, the two predictors with largest positive coefficients at the optimal penalization are  $H_{io}^i(u)$  and  $H_{oo}^i(u)$ , meaning that lawyers with partner status are more likely to advise people who also advise others. In contrast, the  $d_i(u)$  predictor is not one of the first selected, which implies that it is not *how many one advises* but rather *who one advises* that is correlated with partner status. Finally, the two predictors with the largest negative coefficients at the optimal penalization are  $H_{oi}^i(u)$  and  $H_{oi}^o(u)$ , meaning that partner-status lawyers are less likely to interact with other lawyers with whom they have a same advisor.

## 5.2 Case Study II: Identifying fish in a food web

We next perform a similar network prediction task. Here, the data comes from an entirely different domain (ecology), but we still find that our local directed closure coefficients are effective predictors for identifying node type.

More specifically, we study a food web collected from the Florida Bay [44]. In this dataset, nodes correspond to ecological compartments (roughly, species) and edges represent directed carbon exchange (roughly, who-eats-whom). There is an edge from  $i$  to  $j$  if energy flows from compartment  $i$  to compartment  $j$ . There are 128 total compartments, of which 48 correspond to fish. Our prediction task in this case study is to identify which nodes are fish using basic node-level features. The dataset contains 2,106 edges, of which 268 are between fish; 699 are between non-fish; 648 are from a fish to a non-fish; and 491 are from a non-fish to a fish.

We used the same model selection procedure as in the first case study on the SOC-LAWYER dataset described above. Table 3 lists the accuracy and AUC of the  $\ell_1$ -regularized logistic regression model. We again find that our proposed directed closure coefficients form the best set of predictors for this task. We also find minimal difference in prediction accuracy when including degree

features, indicating that the degree features provide little predictive information beyond the directed closure coefficients.

In fact, the regularization path shows that the two closure coefficients  $H_{oo}^o(u)$  and  $H_{oi}^o(u)$  are the most important predictors for identifying fish (Fig. 9), the former being positively correlated with the fish type and the latter positively correlated with the non-fish type. The type of closure associated with the coefficient  $H_{oo}^o(u)$  has previously been identified as important for the network dynamics of overfishing [4], so it is feasible that this predictor is important.

## 6 CONCLUSION

Triadic closure and clustering are fundamental properties of complex networks. Although these concepts have a storied history, only recently have there been local closure measurements (for undirected graphs) that accurately reflect the “friend of friend” mechanism that dominates discussions of closure. In this paper, we have extended the subtle definitional difference of initiator-based vs. center-based clustering to directed networks, where clustering in general has received relatively little attention. We observed a seemingly counter-intuitive result that the same induced triadic structure can produce two different average directed closure coefficients; however, this asymmetry is understandable through our analysis of closure coefficients within a configuration model, which points to the role of moments of the in- and out-degree distributions. Additional analysis showed that this asymmetry can be arbitrarily large.

One of the benefits of new local network measurements is that they can be used as predictors for statistical inference on networks. We demonstrated through two case studies that our directed closure coefficients are good predictors at identifying node types in two starkly different domains—social networks and ecology—achieving over 92% mean AUC in both cases. Furthermore, directed closure coefficients are much better predictors than generalizations of clustering coefficients to directed graphs for these tasks. We anticipate that closure coefficients will become a useful tool for understanding the basic local structure of directed complex networks.

## ACKNOWLEDGMENTS

This research has been supported in part by an ARO Young Investigator Award, NSF Award DMS-1830274, and ARO Award W911NF-19-1-0057.

## REFERENCES

- [1] S. E. Ahnert and T. M. A. Fink. 2008. Clustering signatures classify directed networks. *PRE* 78, 3 (2008). <https://doi.org/10.1103/physreve.78.036112>
- [2] Lars Backstrom, Dan Huttenlocher, Jon Kleinberg, and Xiangyang Lan. 2006. Group formation in large social networks: membership, growth, and evolution. In *KDD*. ACM.
- [3] Brian Ball and Mark EJ Newman. 2013. Friendship networks and social status. *Network Science* 1, 1 (2013).
- [4] Jordi Bascompte, Carlos J Melián, and Enric Sala. 2005. Interaction strength combinations and the overfishing of a marine food web. *PNAS* 102, 15 (2005).
- [5] Stefano Boccaletti, Vito Latora, Yamir Moreno, Martin Chavez, and D-U Hwang. 2006. Complex networks: Structure and dynamics. *Phys. Rep.* (2006).
- [6] Michael J Brzozowski and Daniel M Romero. 2011. Who Should I Follow? Recommending People in Directed Social Networks.. In *ICWSM*.
- [7] Ningyuan Chen and Mariana Olvera-Cravioto. 2013. Directed random graphs with given degree distributions. *Stochastic Systems* 3, 1 (2013).
- [8] James A Davis and Samuel Leinhardt. 1967. The structure of positive interpersonal relations in small groups. (1967).
- [9] Giorgio Fagiolo. 2007. Clustering in complex directed networks. *PRE* 76, 2 (2007).

- [10] Santo Fortunato. 2010. Community detection in graphs. *Phys. Rep.* (2010).
- [11] Bailey K. Fosdick, Daniel B. Larremore, Joel Nishimura, and Johan Ugander. 2018. Configuring Random Graph Models with Fixed Degree Sequences. *SIAM Rev.* 60, 2 (2018). <https://doi.org/10.1137/16m1087175>
- [12] Jerome Friedman, Trevor Hastie, and Rob Tibshirani. 2010. Regularization paths for generalized linear models via coordinate descent. *Journal of statistical software* 33, 1 (2010).
- [13] Johannes Gehrke, Paul Ginsparg, and Jon Kleinberg. 2003. Overview of the 2003 KDD Cup. *ACM SIGKDD Explorations Newsletter* 5, 2 (2003).
- [14] David F Gleich and C Seshadhri. 2012. Vertex neighborhoods, low conductance cuts, and good seeds for local community methods. In *KDD*.
- [15] Catherine Greenhill. 2014. The switch Markov chain for sampling irregular graphs. In *SODA*.
- [16] Keith Henderson et al. 2012. RolX: structural role extraction & mining in large graphs. In *KDD*.
- [17] George C Homans. 1950. The human group. (1950).
- [18] Hong Huang, Jie Tang, Sen Wu, Lu Liu, et al. 2014. Mining triadic closure patterns in social networks. In *WWW*. ACM.
- [19] Matthew O Jackson and Brian W Rogers. 2007. Meeting strangers and friends of friends: How random are social networks? *American Economic Review* 97, 3 (2007).
- [20] Marcus Kaiser. 2008. Mean clustering coefficients: the role of isolated nodes and leafs on clustering measures for small-world networks. *New J. Phys.* (2008).
- [21] Timothy LaFond, Jennifer Neville, and Brian Gallagher. 2014. Anomaly detection in networks with changing trends. In *ODD<sup>2</sup> Workshop*.
- [22] Emmanuel Lazega et al. 2001. *The collegial phenomenon: The social mechanisms of cooperation among peers in a corporate law partnership*. Oxford University Press.
- [23] Jure Leskovec et al. 2010. Signed networks in social media. In *CHI*.
- [24] Jure Leskovec, Jon Kleinberg, and Christos Faloutsos. 2005. Graphs over time: densification laws, shrinking diameters and possible explanations. In *KDD*.
- [25] Jure Leskovec, Kevin J Lang, Anirban Dasgupta, and Michael W Mahoney. 2009. Community structure in large networks: Natural cluster sizes and the absence of large well-defined clusters. *Internet Mathematics* 6, 1 (2009).
- [26] Wei Liao, Jurong Ding, Daniele Marinazzo, Qiang Xu, Zhengge Wang, Cuiping Yuan, Zhiqiang Zhang, Guangming Lu, and Huaifu Chen. 2011. Small-world directed networks in the human brain: Multivariate Granger causality analysis of resting-state fMRI. *NeuroImage* 54, 4 (2011). <https://doi.org/10.1016/j.neuroimage.2010.11.007>
- [27] Tiancheng Lou, Jie Tang, John Hopcroft, Zhanpeng Fang, and Xiaowen Ding. 2013. Learning to predict reciprocity and triadic closure in social networks. *TKDD* 7, 2 (2013).
- [28] Shmoolik Mangan et al. 2003. The coherent feedforward loop serves as a sign-sensitive delay element in transcription networks. *J. of molecular biology* 334, 2 (2003).
- [29] Ron Milo, Shai Shen-Orr, Shalev Itzkovitz, Nadav Kashtan, Dmitri Chklovskii, and Uri Alon. 2002. Network motifs: simple building blocks of complex networks. *Science* 298, 5594 (2002).
- [30] Camelia Minoiu and Javier A. Reyes. 2013. A network analysis of global banking: 1978–2010. *Journal of Financial Stability* 9, 2 (2013). <https://doi.org/10.1016/j.jfs.2013.03.001>
- [31] Michael Molloy and Bruce Reed. 1995. A critical point for random graphs with a given degree sequence. *Random structures & algorithms* 6, 2-3 (1995).
- [32] Mark EJ Newman, Stephanie Forrest, and Justin Balthrop. 2002. Email networks and the spread of computer viruses. *PRE* 66, 3 (2002).
- [33] Mark EJ Newman, Steven H Strogatz, and Duncan J Watts. 2001. Random graphs with arbitrary degree distributions and their applications. *PRE* (2001).
- [34] Mark E J Newman. 2003. The structure and function of complex networks. *SIAM Rev.* (2003).
- [35] Jukka-Pekka Onnela, Jari Saramäki, János Kertész, and Kimmo Kaski. 2005. Intensity and coherence of motifs in weighted complex networks. *PRE* 71, 6 (2005).
- [36] Pietro Panzarasa, Tore Opsahl, and Kathleen M Carley. 2009. Patterns and dynamics of users' behavior and interaction: Network analysis of an online community. *J. Assoc. Inf. Sci. Technol.* (2009).
- [37] A Ramachandra Rao, Rabindranath Jana, and Suraj Bandyopadhyay. 1996. A Markov chain Monte Carlo method for generating random (0, 1)-matrices with given marginals. *Sankhyā: The Indian Journal of Statistics, Series A* (1996).
- [38] Anatol Rapoport. 1953. Spread of information through a population with socio-structural bias: I. Assumption of transitivity. *The Bull. of Math. Biophysics* (1953).
- [39] Matthew Richardson, Rakesh Agrawal, and Pedro Domingos. 2003. Trust management for the semantic web. In *International semantic Web conference*. Springer.
- [40] Pablo Robles, Sebastian Moreno, and Jennifer Neville. 2016. Sampling of attributed networks from hierarchical generative models. In *KDD*.
- [41] Daniel Romero and Jon Kleinberg. 2010. The directed closure process in hybrid social-information networks, with an analysis of link formation on Twitter. In *ICWSM*.
- [42] Comandur Seshadhri, Tamara G Kolda, and Ali Pinar. 2012. Community structure and scale-free collections of Erdős-Rényi graphs. *PRE* (2012).
- [43] C. Seshadhri, Ali Pinar, Nurcan Durak, and Tamara G. Kolda. 2016. Directed Closure Measures for Networks with Reciprocity. *J. of Complex Networks* (2016).
- [44] C. Bondavalli Ulanowicz, R.E. and M.S. Egnatovich. 1998. *Network Analysis of Trophic Dynamics in South Florida Ecosystem*. Technical Report CBL 98-123.
- [45] Stanley Wasserman and Katherine Faust. 1994. *Social network analysis: Methods and applications*. Vol. 8. Cambridge university press.
- [46] Duncan J Watts and Steven H Strogatz. 1998. Collective dynamics of 'small-world' networks. *Nature* (1998).
- [47] Zhi-Xi Wu and Petter Holme. 2009. Modeling scientific-citation patterns and other triangle-rich acyclic networks. *PRE* (2009).
- [48] Hao Yin, Austin R Benson, and Jure Leskovec. 2019. The local closure coefficient: a new perspective on network clustering. In *WSDM*.
- [49] Hao Yin, Austin R Benson, Jure Leskovec, and David F Gleich. 2017. Local higher-order graph clustering. In *KDD*.